TC
Posta 6

Proceedings of ICONE 8
8th International Conference on Nuclear Engineering
April 2-6, 2000, Baltimore, MD USA

ICONE-8036

A NEW NEURAL NETWORK CONCEPT FOR CONTROL OF NUCLEAR REACTOR SYSTEMS

Benedito Dias Baptista Filho
Instituto de Pesquisas Energeticas e Nucleares
IPEN-CNEN/SP – RTH - Cx. Postal 11049
CEP 05598-900 - São Paulo – SP – Brazil
FAX +55 11 816-9432
E-mail: bdbfilho@net.ipen.br

Eduardo Lobo Lustosa Cabral
Escola Politécnica da Universidade de São Paulo
Phone +55 11 818-5575 (212)
FAX +55 11 813-1886
E-mail: elcabral@usp.br

Keywords: **NEURAL NETWORKS, CONTROL SYSTEMS, NATURAL CIRCULATION**

ABSTRACT

In this work the novel approach to artificial neural networks based on the design of task-specific networks and on a neuron model with multiple synapses developed by Baptista, Cabral and Soares (1998) is extended to accommodate external perturbations. As an example of this new development the neural network is applied to control the fluid temperature of a natural circulation loop. The learning and the action processes are made through simulations. The natural circulation loop simulation model is based on physical equations and on experimentally identified parameters. The results show that besides the excellent learning capability and generalization, the new improvements are suitable to accommodate external perturbations so that the network is able to maintain the controlled variable within allowable limits even in the presence of strong perturbations.

INTRODUCTION

The purpose of this work is to present new developments associated with a new concept of artificial neural networks which was introduced by Baptista, Cabral and Soares (1998) and Baptista (1998). This new neural network concept, now nominated MULSY Neural Network (Multiple Synapses N.N.), is based on the design of task specific neural networks and on the physiology of biological neural systems. Baptista, Cabral and Soares developed a basic neural network control unit which was used to control a planar two-link manipulator. This control unit is improved here to deal with external perturbations that affect the control task.

In this work a thermal-hydraulic system is used as the control object. This system consists on a Natural Circulation Loop (NCL) which resembles an Advanced Pressurized Water Reactor Decay Heat Removal System. The NCL problem is very non-linear and due to the complexity of its functions it represents a difficult control problem. Comparing the NCL with a manipulator arm both are non-linear but their dynamic behavior is quite different, the NCL is more complex but it is much slower than the manipulator. In this work a system of different nature was chosen to show the capability of the MULSY Neural Network to deal with different kinds of problems.

This paper consists of six sections. The first section is this introduction. The second section reviews the basic principles of the MULSY concept. The third section shows the Natural Circulation Loop and the dynamic model used to simulate it. The fourth section presents the application of the MULSY in the control of the NCL and the new developments and improvements added to the basic control unit. The fifth section is devoted to show the results. The sixth section presents the conclusions.

MULSY CONCEPT

The present ANNs consider regular arrays of units (representing neurons) interconnected by single connections with linking weights (representing synapses). In the last years ANN's researchers have focused on the limitations of this approach. Kolen and Goel (1991) concluded that current connectionist methods may be too limited for the task of learning they seek to solve, and they proposed that the development of task-specific methods may enhance the power of neural networks.

Baptista., Cabral and Soares (1998) have developed the MULSY Neural Network based on the following principles: 1) an ANN design shall be based on biological systems to take the profit of their evolutionary nature; 2) it shall represent what it

7703
724

knows and what is to learn and it must have capabilities to generalization, therefore it must have different regions specialized for different functions; 3) it must be robust to missing information, incorrect data and unit removal or malfunction; 4) the learning task shall be done in real-time while functioning and shall be independent on the initial unit strength; and, 5) the process of learning and functioning must be computationally efficient without limiting the power of connection's transfer functions to obtain higher classes of input-to-output functions.

Figure 1 presents the "motor control unit", which the MULSY Network is based on as developed by Baptista., Cabral and Soares (1998). The input pathway from the upper level system ("The Wish" - I_c) and that from the sensory system ("The Actual Condition" - I_s) converge to the unit responsible for sensing the actual error (ε) and to the motor unit. This resembles the architectural design and flow of information present in biological neuronal circuits as described by Kandel, Schwartz and Jessel (1991).

To model the biological function of a pool of neurons, it is enough a single unit with a transfer function in a scaled positive/negative domain to emulates agonist and antagonist circuits. The transfer function chosen is the modified hyperbolic tangent function expressed as,

$$O = T_N \tanh\left(\alpha \sum S\right), \qquad (1)$$

where, O is the output signal, T_N represents the "size" of the unit, α is a gain, and ΣS is the summation of all synaptic input to that unit. The "size" can be set to convenient values to improve the linearity in the range of interest or to amplify or reduce the input to output relation.

The signals are transmitted to the neural units through connections (synapses) that are modeled by the following expression:

$$S = \frac{T}{1 + a(I - I_0)^2}, \qquad (2)$$

where, T is the "strength" of the synapse, which can be set as any positive value (excitatory) or as any negative value (inhibitory), a is a constant that can be adequately choose to produce smooth functions according to the number of synapses, I is the signal value that pass through the axon, and I_0 (which is called here "threshold") is the value of I that maximizes S, the output value to the target cell. This function is much simpler than sigmoidal functions in terms of computational time and permits amplification and selective response. With convenient strengths and thresholds, a set of these functions can produce any kind of continuous function.

The wish and the actual condition signals are linked to the error sense unit with rigid connections (synapses) that will not change with training. These connections are modeled to make the error unit to sense the actual condition from the sensory system with the opposite sign of the wish signal, i.e., $\varepsilon = I_c - I_s$.

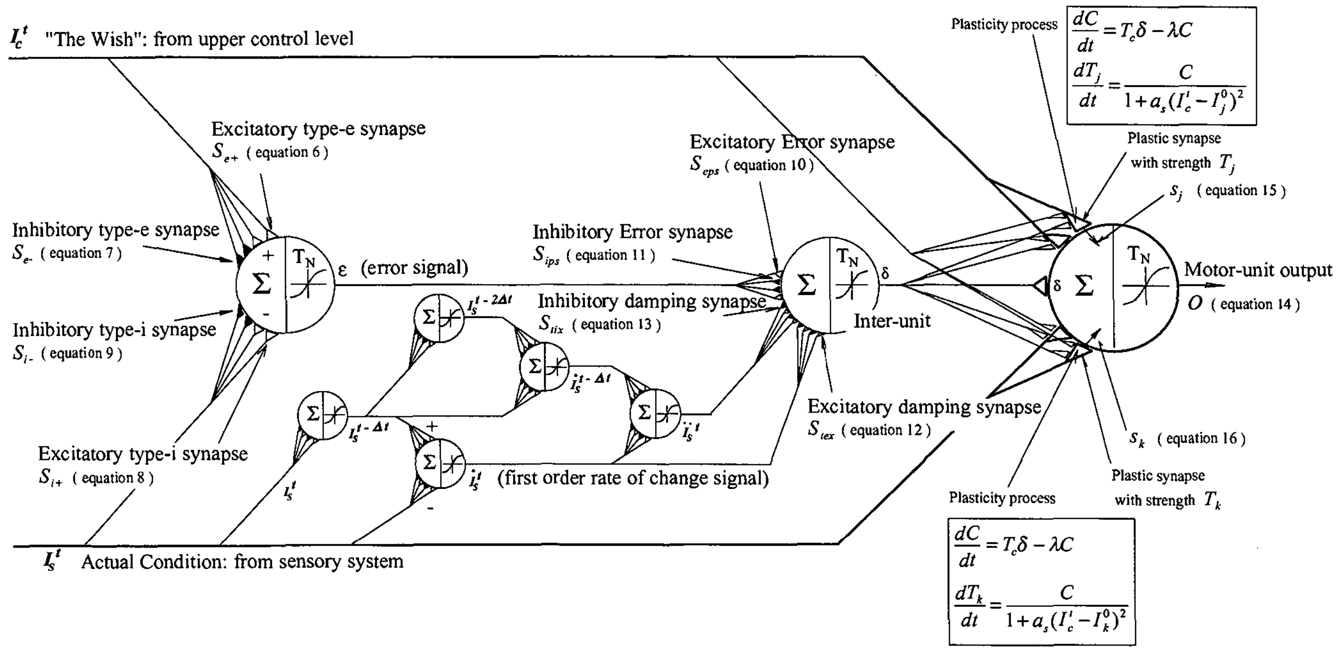

Figure 1 - Motor Control Unit of the MULSY Neural Network as developed by Baptista., Cabral and Soares (1998).

The schema of multiple branches of synaptic terminals improves the reliability as long as it allows the increase in the number of terminals, what can make a more fail-proof system. Equations (3) through (6), which model the terminal types' S_{e+}, S_{e-}, S_{i+} and S_{i-}, indicated in Fig. 1, are based on the model of a single synapse.

$$S_{e+} = \frac{1}{N}\left(\frac{2}{1+0.25(I-2)^2}\right); \quad (3)$$

$$S_{e-} = \frac{1}{N}\left(\frac{2}{1+0.25(I+2)^2}\right); \quad (4)$$

$$S_{i+} = \frac{1}{N}\left(\frac{-2}{1+0.25(I+2)^2}\right); \quad (5)$$

$$S_{i-} = \frac{1}{N}\left(\frac{-2}{1+0.25(I-2)^2}\right); \quad (6)$$

where, N is the number of redundancies, which does not modify the net result, the subscript e refers to the excitatory synapses, and the subscript i refers to the inhibitory synapses.

The rate of change of the sensory signals is sensed by the differences between signals from units in different layers. The inter-units responsible for this function are presented between the error signal and the actual condition signal of Fig. 1. These units are coupled with rigid connections, which do not change during training. The output signals of these units in the several levels represent the rates of change of sensory signals. These signals are equivalent to the rate of change of the error signal when the desired value is constant. These signals are combined to the error signal into one intermediate unit that makes the connections with the output unit. This signal combination represents the system dynamics as an analogy to the summation of $a_0\ \varepsilon + a_1\ d\varepsilon / dt + a_2\ d^2\varepsilon / dt^2 + \ldots$ The coefficient a_0 of the error was implemented by the following synaptic functions that result in a linear transfer function:

$$S_{eps} = \frac{1}{N}\left(\frac{T_\varepsilon}{1+0.25(I-2)^2}\right); \quad (7)$$

$$S_{ips} = \frac{1}{N}\left(\frac{-T_\varepsilon}{1+0.25(I+2)^2}\right); \quad (8)$$

where T_ε is the strength of the error synapse.

The synaptic transfer functions for the connections of the rate of change of the sensory signals with the inter-unit are modeled with damping characteristics of the type of $x/x/$. This is necessary to attenuate oscillations and to make the process stable even in the presence of high rates of change. Equations (9) and (10) implement the coefficients a_i according to that characteristic.

$$S_{tex} = \frac{1}{N}\left(\frac{T_r}{1+11(I-1)^2}\right); \quad (9)$$

$$S_{tix} = \frac{1}{N}\left(\frac{-T_r}{1+11(I+1)^2}\right); \quad (10)$$

where T_r is the strength of the rate of change synapses.

The sensory, the upper level, the error and the sensory rates of change signals converge to the output unit, whose output signal (O) will be the input to the actuator's drive. Then the output unit receives sensory information, upper level commands, and a combination of error and rates of change of the signals, and generates the output signal according to the following equation,

$$O = T_N \tanh\left[\alpha\left(\delta + \sum S_j + \sum S_k\right)\right], \quad (11)$$

where S_j and S_k are the outputs of the upper level and sensory motor unit synapses respectively, and δ is the signal generated in the inter-unit as a function of the error and rates of change.

The sensory and upper level signals are transmitted through two symmetrical (in terms of threshold and strength) sets of synapses, which are the synapses with plasticity that will be adjusted by learning. Equations (12) and (13) represent these plastic synapses. This solution maintains similitude with the mechanisms of sensitization, habituation and classical conditioning, as described by Kandel, Schwartz and Jessel (1998).

$$S_j = \frac{T_j}{1+a(I_c - I_{0,j})^2}; \quad (12)$$

$$S_k = \frac{T_k}{1+a(I_s - I_{0,k})^2}; \quad (13)$$

where S_j is the output of the j-th synapse connected with "the wish", S_k is the output of the k-th synapse connected with the actual condition signal, T_j and T_k are the strength of the j-th and of the k-th synapses respectively.

The action of the facilitating inter-unit over the presynaptic contacts of the motor unit (the learning cell) is to increase a source term that acts on the long-term plasticity. This is done through a cumulative process, expressed by the following equation:

$$\frac{dC}{dt} = T_c\delta - \lambda C, \quad (14)$$

where, C is a long-term change's trigger factor, δ is the output signal of the facilitating inter-unit, λ is a decay constant, and,

T_c is the strength of the facilitating synapse (that controls the rate of change).

According to equation (14) the long-term change's trigger factor (C) can grow in a rate proportional to the learning signal (δ) up to an equilibrium value. This makes the change in the synapses strength faster or slower. If the incoming learning signal decreases to zero the long-term change's trigger factor will also decrease to zero, according to the rate established by the decay constant (λ). This means that after a reasonable period of training, when there are no error and no excessive movement, there will be no need for further changes, thus making the process inherently stable. To complete this idea, it is necessary to set an artifice that makes the changes occurring mainly in the convenient synapses, i.e., in the synapses where the threshold (I_0) is closer to the incoming desired values, like in the resonance hypothesis of Paul Weiss (1948). This characteristic makes the correct synaptic selection. In equation (15) the rate of change of the strength of the motor unit synapses (parameter T_j or T_k in equations 12 and 13) is a function of the long-term change's trigger factor and of the synaptic threshold.

$$\frac{dT_{j/k}}{dt} = \frac{C}{1 + a_s(I_c^t - I_{0,j/k})}, \tag{15}$$

where, $T_{j/k}$ is the strength of the j/k-th synapse of the motor unit, a_s is the constant of the Gaussian like function of the facilitating synapse, I_c^t is the signal value that comes from the upper control level (the Wish), and $I_{0,j}$ is the threshold of the synapse.

In summary, equation (14) emulates a cumulative process within the synaptic terminal which generates a source term that is the trigger of the long term changes, and equation (15) selects the correct synaptic terminal which generates the rate of change of the synaptic strength. This process acts on all synaptic contacts in the target unit but, with a higher growing rate in the synapses that have the threshold closer to the input desired signal ($I \approx I_{0,j}$). Before any training the plastic synapses have no strength, i.e., $T_{j/k} = 0$. The existence of an error signal ε yields a δ signal different from zero that acts to increase or to decrease the long-term trigger factor C given by equation (14). The plastic changes, responsible for the learning process, take place in the motor unit synapses. The synapse's strength changes according to equation (15). The dotted line in Fig. 1 indicates that I_c is used to provide the selective characteristic of the learning process. Thus, the wish signal is used to control the plastic change of both motor unit synapse sets to guarantee the symmetry between them.

NATURAL CIRCULATION LOOP – THE CONTROL PROBLEM

Fig. 2 presents a schematic of the Natural Circulation Loop (NCL) which resembles an Advanced Pressurized Water Reactor Decay Heat Removal System. The NCL has an electric heater, that it is the hot source of the system, and a heat exchanger, that is the heat sink. The heat exchanger is made of two horizontal manifolds connected by a vertical tube bundle immersed in a water tank. Cold water coming from a elevated water reservoir is supplied to the water tank by gravity. A magnetic flow meter is installed in the main circuit line. The secondary cooling water flow is controlled by a globe valve with the aid of a flow meter.

A numerical model, described in Appendix A, was developed to simulate the thermal and hydraulic processes of the NCL. Fig. 2 also presents some conventions used in the simulation model. Tables 1 and 2, inside Fig. 2, show the parameters used in the model. A description of these parameters is found in Appendix A

The coupling of the NCL Model with MULSY Network

The NCL control problem consists on the control of the primary water temperature at a given position in the loop, acting only on the heater power. The secondary side water temperature and flow rate are assumed to be disturbances to the process, and they should be monitored by the neural network controller to adjust the magnitude of the power control signal. The solution of this problem requires an improvement of the Motor Control Unit of the MULSY Network presented in Section II.

To manage the external disturbances the MULSY Network is modified to receive beyond the desired and actual temperature signals, the secondary water inlet temperature and the cooling water valve flow area fraction. Note that these signals are all scaled to the range of –1 to +1. Fig. 3 shows the MULSY network with these modifications. In this new configuration, the control motor unit of Fig. 1 is linked to two parallel branches which processes the disturbances signals. Each one of these branches has a set of plastic synapses. The expressions of these plastic synapses are exactly the same as the ones used for the wish and the actual signals, eq. (2).

The δ signal, composed by the combination of the error with the rate of change of the controlled temperature, is also used to modify the synaptic strength of these new sets of plastic synapses. The desired signal, I_c, is also used to provide the selective characteristic for the strength adjustment of these disturbance synapses.

The output of the disturbances units are used to modulate the gain of the motor unit output (O) in order to generate the control signal, as follow:

$$S_c = O_1 O_2 O, \tag{16}$$

where S_c is the control signal and O, O_1 and O_2 are the outputs of the control units of Fig 3

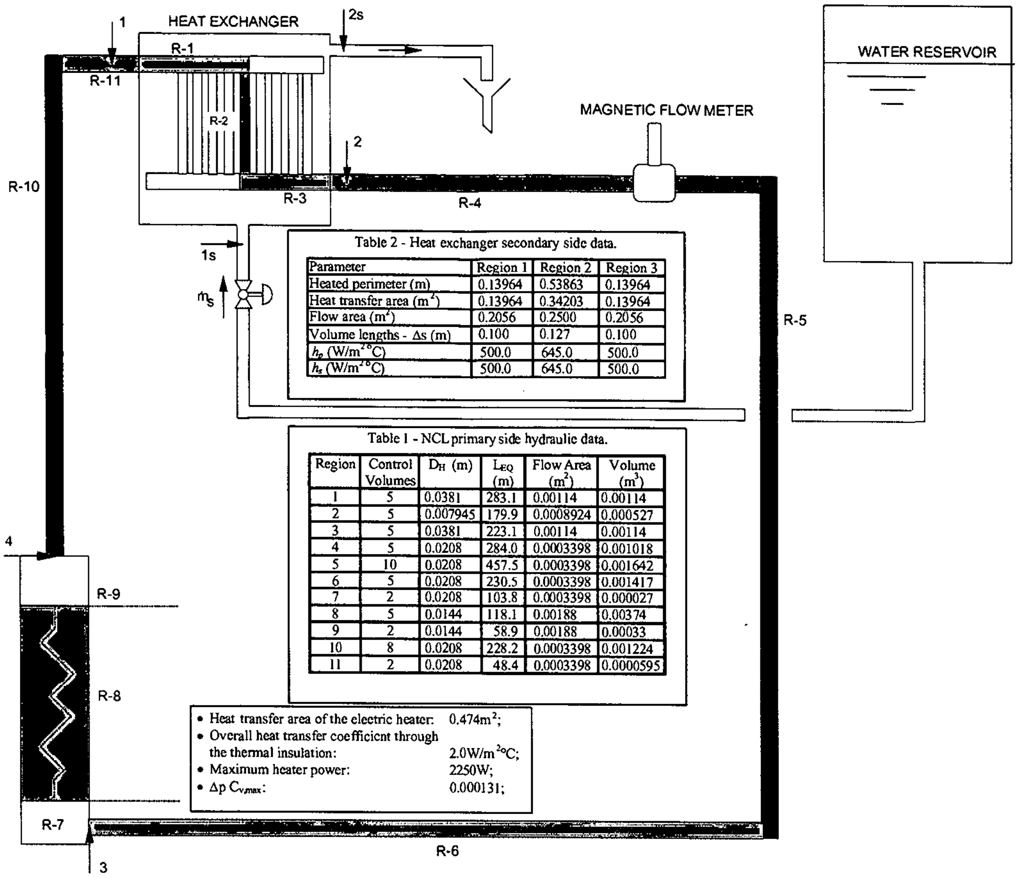

Table 2 - Heat exchanger secondary side data.

Parameter	Region 1	Region 2	Region 3
Heated perimeter (m)	0.13964	0.53863	0.13964
Heat transfer area (m^2)	0.13964	0.34203	0.13964
Flow area (m^2)	0.2056	0.2500	0.2056
Volume lengths - Δs (m)	0.100	0.127	0.100
h_p ($W/m^2 {}^oC$)	500.0	645.0	500.0
h_s ($W/m^2 {}^oC$)	500.0	645.0	500.0

Table 1 - NCL primary side hydraulic data.

Region	Control Volumes	D_H (m)	L_{EQ} (m)	Flow Area (m^2)	Volume (m^3)
1	5	0.0381	283.1	0.00114	0.00114
2	5	0.007945	179.9	0.0008924	0.000527
3	5	0.0381	223.1	0.00114	0.00114
4	5	0.0208	284.0	0.0003398	0.001018
5	10	0.0208	457.5	0.0003398	0.001642
6	5	0.0208	230.5	0.0003398	0.001417
7	2	0.0208	103.8	0.0003398	0.000027
8	5	0.0144	118.1	0.00188	0.00374
9	2	0.0144	58.9	0.00188	0.00033
10	8	0.0208	228.2	0.0003398	0.001224
11	2	0.0208	48.4	0.0003398	0.0000595

- Heat transfer area of the electric heater: $0.474m^2$;
- Overall heat transfer coefficient through the thermal insulation: $2.0W/m^{2o}C$;
- Maximum heater power: 2250W;
- Δp $C_{v,max}$: 0.000131;

Figure 2 - Schema of the Natural Circulation Loop (NCL).

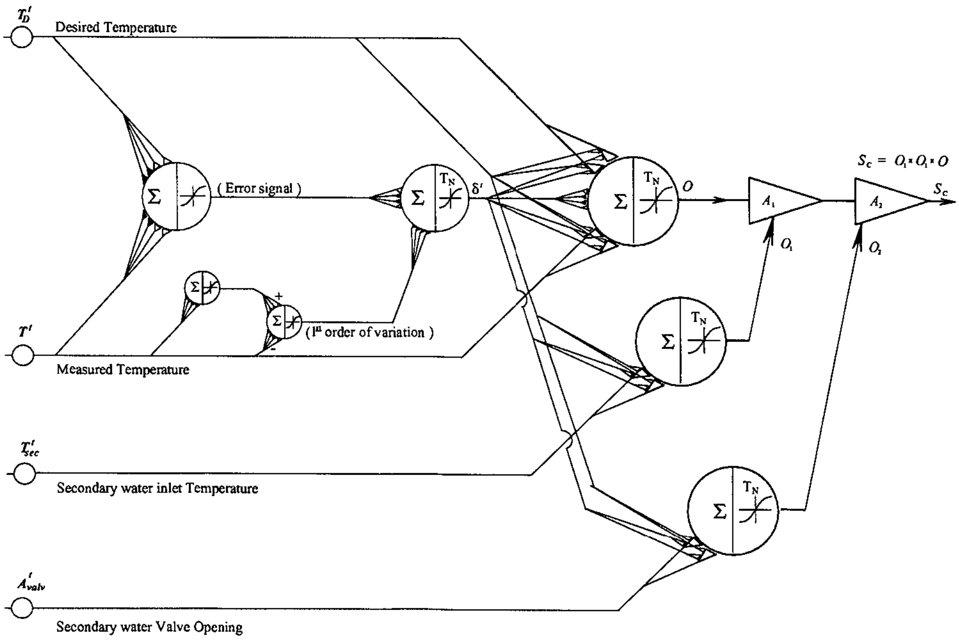

Figure 4 - MULSY Neural Network controller representation.

In this implementation, the network considers only the first order variation of the error signal (1st order approximation). Higher order terms are neglected because of the huge inertia of the NCL. This large inertia, which can be observed in the great time constant of the NCL, eliminates fast variations.

Neural Network Data

Table 3 presents the data used in the MULSY Neural Network of Fig. 3. These data are the same as the ones used in the case of the planar two-link manipulator controller of Baptista, Cabral, and Soares (1998), except by the number of synaptic terminals and the values of some constants. The decay constant for adjustment of the plastic synapses strength, λ, was reduced by a hundred times (from 10 to 0.1) to match with the process time constant, which is very slow for a natural circulation process. As long as a different number of synapses is used, the constant a_s of the facilitating synapses is different, see Baptista. (1998). However, its relationship with the constant a of the plastic synapses is the same, i.e., a_s/a = 144/28.8 = 100/20 = 5. Note that, as it is necessary to turn off the plasticity process in some instances (as it is explained in the item regarding the training) the constant T_C assumes two different values, either 0 or 0.1.

Table 3 - Neural network data.

Parameter	Value
Unit's size - T_N	2.1
Units gain constant - α	0.5
Plastic synapse's constant – a	20.0
Plastic synapses in the sensory to output unit	13
Plastic synapses in the "wish" to output unit	13
Plastic synapses in the disturbance units	13
Consecutive thresholds interval in the plastic synapses ($\Delta I = I_{0,j+1} - I_{0,j}$)	0.2
Strength of error synapses – T_ε	2.5
Strength of rates synapses – T_r	0.09
Strength of facilitating synapses – T_c	0 / 0.1
Synaptic strength decay constant - λ	0.1
Plastic synapse's plastic constant – a_s	100.0

RESULTS

Training phase

The MULSY Network training is performed during the execution of action commands, following an unsupervised training method. Desired temperatures and projected disturbances constitute the training universe. Different from the manipulator's case, there are three training data tables, one for each given variable: the desired temperature, the cooling water valve opening and the inlet cooling water temperature. Tables 4 to 6 show the data sets - note that the training is developed in three stages. The effects of the three variables are not superposed, i.e., while training for one of the variables, the synaptic plasticity process of the branches associated with the others variables is blocked (no-plastic changes). This is done by setting $T_C = 0$.

Each stage of the training phase is divided into sessions, making possible to observe the learning progress. In the 1st stage the seven conditions specified in the Table 4 are submitted for 3 times to the MULSY Network controller. This represented 3x7x14,400 = 302,400 seconds of process time. The 2nd stage consists on the repetition for 2 times the 9 conditions of Table 5, or 2x9x12,800 = 230,400 seconds of process time. In the 3rd and last stage the first session is accomplished with 10,800 seconds for the first condition and 3,600 seconds for each one of the other conditions. The second session considers 7,200 seconds for the first condition and again 3,600 seconds for the others. Thus, the last stage represents 1x10,800 + 1x7,200 + 2x9x3,600 = 82,800 seconds of process time. Therefore, the whole training phase represents a total of 615,600 seconds of simulate process, which is about 171 hours.

Table 4 – Training data for the *desired temperature*

Condition	Duration (s)	T_{env} (°C)	Cooling Temp.	Valve opening	**Desired Temp.**
1	14400.	25.0	20.0	0.25	**30.00**
2	14400.	25.0	20.0	0.25	**35.00**
3	14400.	25.0	20.0	0.25	**40.00**
4	14400.	25.0	20.0	0.25	**45.00**
5	14400.	25.0	20.0	0.25	**50.00**
6	14400.	25.0	20.0	0.25	**55.00**
7	14400.	25.0	20.0	0.25	**25.00**

Table 5 – Training data for the *cooling water temperature perturbation* (stage 2).

Condition	Duration (s)	T_{env} (°C)	**Cooling Temp.**	Valve opening	Desired Temp.
1	12800.	25.0	**14.0**	0.25	50.00
2	12800.	25.0	**16.0**	0.25	50.00
3	12800.	25.0	**18.0**	0.25	50.00
4	12800.	25.0	**20.0**	0.25	50.00
5	12800.	25.0	**22.0**	0.25	50.00
6	12800.	25.0	**24.0**	0.25	50.00
7	12800.	25.0	**26.0**	0.25	50.00
8	12800.	25.0	**28.0**	0.25	50.00
9	12800.	25.0	**30.0**	0.25	50.00

After executing the three training stages, the strength of the synaptic contacts grew from the initial values (zero) to the values shown in Fig. 4 to 6. It took about 1.48h of CPU time in a PENTIUM 166 MHz microcomputer to perform the training phase with a simulated time of 171 hours.

Table 6 - Training data for the va*lve opening perturbation.*

Condition	Duration (s)	T_{env} (°C)	Cooling Temp.	Valve opening	Desired Temp.
1	1x10800 1x7200.	25.0	20.0	**0.05**	50.00
2	2x3600.	25.0	20.0	**0.10**	50.00
3	2x3600.	25.0	20.0	**0.15**	50.00
4	2x3600.	25.0	20.0	**0.20**	50.00
5	2x3600.	25.0	20.0	**0.25**	50.00
6	2x3600.	25.0	20.0	**0.30**	50.00
7	2x3600.	25.0	20.0	**0.35**	50.00
8	2x3600.	25.0	20.0	**0.40**	50.00
9	2x3600.	25.0	20.0	**0.45**	50.00
10	2x3600.	25.0	20.0	**0.50**	50.00

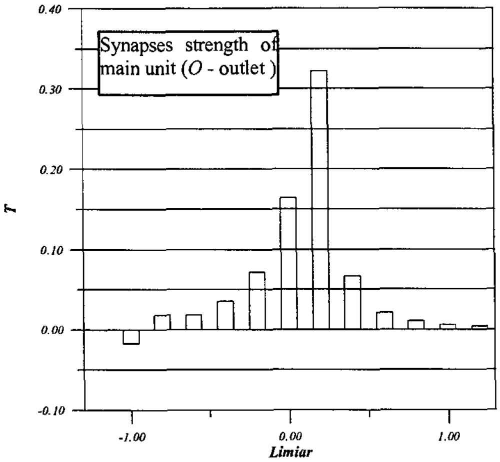

Figure 4 - Synaptic strengths after the 1st training stage.

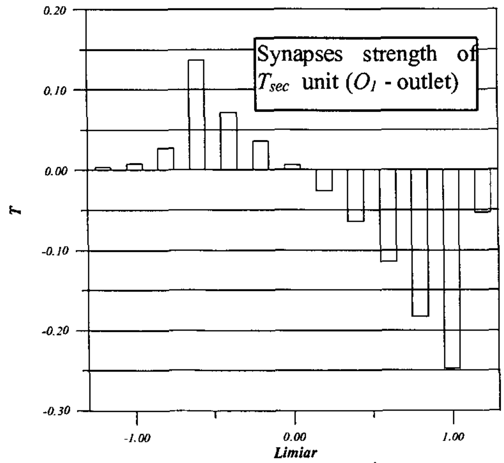

Figure5 - Synaptic strengths after the 2nd training stage.

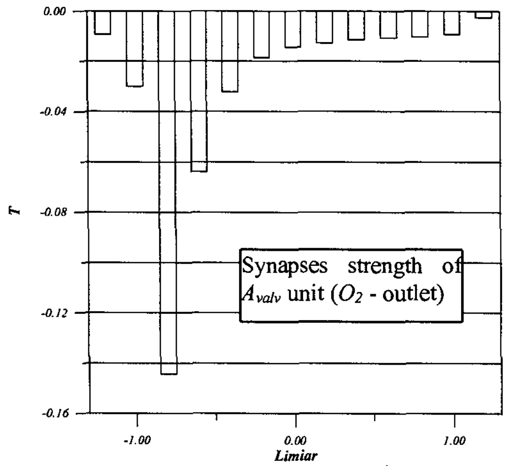

Figure 6 - Synaptic strengths after the 3rd training stage.

Performance Tests

After the training, the MULSY Network controller is able to control the NCL primary water temperature under several conditions of disturbances in the cooling water valve opening and in the cooling water temperature. Tests are performed to evaluate the generalization capacity of the network to execute commands that are not present in the training tables. During these tests, the plasticity mechanisms are blocked to avoid additional synaptic strength modification. The tests are executed on the physically possible domain, limited by the plant design.

The results of a single simulation test composed of several transient operations within a 26 hours period are presented. The test begins with the environmental temperature at 25°C and the cooling water temperature at 20°C. In the first command the desired primary side temperature is equal to the mean training conditions, i.e., 50°C at the heater outlet, with the cooling water valve opening corresponding to 25%. The test continues with the conditions shown in Table 7.

Table 7 - Performance test data set.

Condition	Duration (s)	T_{env} (°C)	Cooling Temp.	Valve Opening	Desired Temp.
1	16000.	25.0	20.0	0.25	50.00
2	7200.	25.0	23.0	0.25	50.00
3	7200.	25.0	25.0	0.25	50.00
4	7200.	25.0	25.0	0.25	55.00
5	7200.	25.0	25.0	0.12	55.00
6	7200.	25.0	25.0	0.08	55.00
7	7200.	25.0	25.0	0.08	60.00
8	7200.	25.0	25.0	0.08	33.00
9	7200.	25.0	15.0	0.08	33.00
10	7200.	25.0	15.0	0.08	53.00
11	7200.	25.0	15.0	0.08	42.00
12	7200.	25.0	17.0	0.33	37.00

The duration of the first condition was chosen to allow the NCL primary water temperature to approach almost a steady state condition. The natural circulation process in the NCL requires approximately 22,000 seconds (experimentally measured) to reach a steady state condition in the heat exchanger secondary side. Note that 16,000 seconds is about the time to reach partial regime stability in the primary side of the heat exchanger, therefore this is the duration chosen for the first step. All the other steps last 7,200 seconds, which is about 1/3 of the time to reach stabilization, this leads to about 95% of the steady state primary side temperature. Fig. 7 shows the tests conditions as a percentage of the mean training conditions (primary water temperature of 50°C, cooling water temperature of 20°C and valve opening fraction of 0.25). Observe that some values of Table 7 are out of the training set range, others are between two training values but not coincident with any one.

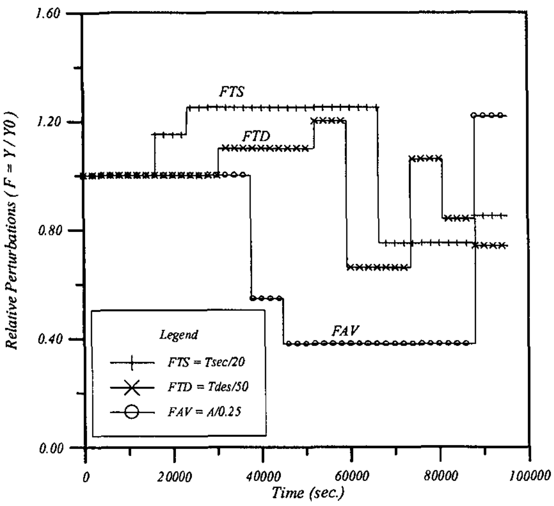

Figure 7 - Relative Perturbations.

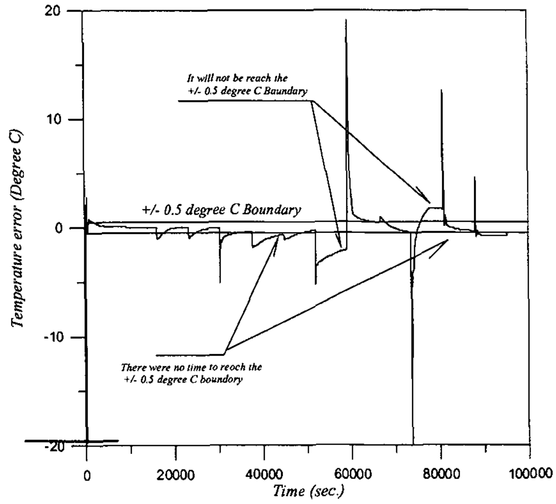

Figure 8 - Temperature error evolution.

It took about 16 minutes and 35 seconds of CPU time in a PENTIUM 166 MHz computer to perform the tests of Table 7, which represents 95,200 seconds of simulated process time.

The error in the desired temperature, defined as the difference between the observed and desired temperatures is presented in Fig. 8. Only in four conditions the observed temperature errors are over the range of ±0.5°C. Two of these conditions happen when the time was not enough for the system to accommodate the perturbation. Another condition happens when the two highest perturbations (cooling water temperature of 15°C and valve opening of 0.08) are combined. The last condition happened when the valve opening of 0.08 is combined with a desired temperature 5°C over the maximum trained temperature.

CONCLUSIONS

As it was demonstrated by Baptista, Cabral, and Soares (1998), the option of task-specific networks with the use of multiple contacts in the axon terminals increases the integration capability of the network. Higher classes of connection's (synapse) transfer functions improve the input-to-output relation, allowing a reduction in the total number of units with expensive sigmoidal functions. The training task is performed without the need of input-output examples, allowing on-line training during the execution of desired commands, as in an *unsupervised learning approach.*

In this work an improvement in the MULSY Neural Network concept to accommodate external perturbations is presented. The results obtained in the NCL temperature control, even with perturbation conditions outside the training set, show that the MULSY Network is able to generalize the learning. The good performance indicates that the MULSY Network with this disturbance rejection scheme can be easily implemented in the control of any kind of system.

ACKNOWLEDGMENTS

The authors acknowledge the financial support given by Fundação de Amparo à Pesquisa do Estado de São Paulo (FAPESP) to present this paper.

REFERENCES

Baptista F., B.D.., Cabral, E.L.L. and Soares, A.J., 1998, "A New Approach to Artificial neural Networks," *IEEE Transactions on neural Networks, Vol. 9, No. 6, pp. 1167-1179.*

Baptista F., B. D., ***Neural Networks for Control of Nuclear Reactor Systems***, São Paulo: 1998, Thesis (Doctoral) – Instituto de Pesquisas Energéticas e Nucleares (in portuguese).

Kolen, J.F. and Goel, A.K., 1991, "Learning in Parallel Distributed Processing Networks: Computational Complexity and Information Content", *IEEE Transactions on Systems, Man, and Cybernetics, Vol. 21, No. 2.*

Kandel, E.R., Schwartz, J.H. and Jessel, T.M., 1991, *Principles of Neural Science*, Prentice-Hall International Inc., Third Edition.

Weiss, P., and Hiscoe, H.B., 1948, "Experiments on the mechanism of nerve growth", *J. Exp. Zool., 107:315-395.*

APPENDIX A – THE NCL MODEL

This Appendix presents the numerical model used to simulate the thermal-hydraulic processes of the NCL. Although the model is simple it is able to adequately simulate the dynamics of the NCL. The basic assumptions used in the model are one-dimensional flow and incompressible fluid.

A. Mass Conservation

For the mass conservation equation the water is considered an incompressible fluid. Thus, for one-dimensional flow, the mass conservation results in a constant mass flow rate throughout the whole loop at any instant. This result allows to decouple the continuity and momentum equations from the energy equation.

B. Energy Conservation

In the energy balance the dissipation terms and the heat conduction through the water are neglected, so that the general energy equation for the fluid in a control volume is given by:

$$\rho A\frac{\partial T}{\partial t} = -\dot{m}C\frac{\partial T}{\partial s} - Pq'' , \qquad (17)$$

where ρ is the average water density in the volume, C is the water specific heat at constant pressure, T is the temperature, A is the flow area, $\dot{m}$ is the mass flow rate, s represents the dimension in the flow direction, P is the section perimeter, and q'' is the heat flux.

To distinguish between the two fluids in the heat exchanger, the water in the main loop is called *primary fluid* and the cooling water in the heat exchanger is called *secondary fluid.* With this convention the energy equation is applied to the NCL as described next.

The NCL is divided into regions. These regions are presented in Fig. 2, for example region 4 is denoted by R-4. Each region is further divided into several volumes. The general energy equation applied to the primary side results in following expression:

$$\rho_{r,i}V_{p,r,i}C\frac{\partial T_{p,r,i}}{\partial t} = -\dot{m}_p C\Delta s\frac{\partial T_{p,r,i}}{\partial s} - S_{p,r,i}q''_{p,r,i} , \qquad (18)$$

where the subscript r defines the region, the subscript i denotes the volume, the subscript p specifies the primary side, Δs is the volume length, and S is the volume surface area. For the secondary side of the heat exchanger the energy equation is similar.

The coupling between the primary and secondary fluids is made by the heat transfer across the tube walls of the heat exchanger. An energy balance in the tube walls results in the following expression:

$$\rho_M V_M C_M\frac{\partial T_{M,r,i}}{\partial t} = S_{p,r,i}q''_{p,r,i} + S_{s,r,i}q''_{s,r,i} , \qquad (19)$$

where the subscript M denotes the metal and, q''_p and q''_s are the wall heat fluxes at the primary and secondary sides respectively. These heat fluxes are given by the following equations:

$$q''_{p,r,i} = h_{p,r,i}(T_{p,r,i} - T_{M,r,i}) ; \qquad (20)$$

$$q''_{s,r,i} = h_{s,r,i}(T_{M,r,i} - T_{s,r,i}) ; \qquad (21)$$

where h_p is the heat transfer coefficient from the primary fluid to the tube wall, h_s is the heat transfer coefficient from the tube wall to the secondary fluid, and T_M is the temperature of the metal of the tubes. These heat transfer coefficients are obtained experimentally.

For the regions inside the electric heater, the heat generated by the electric resistance is completely transferred to the water, so that the term $S_{p,r,i}q''_{p,r,i}$ represents the fraction of the electric heat generated inside the volume i. For the others primary side regions, the heat flux corresponds to the heat loss to the environment, which is calculated according to eq. 20 and the next expression:

$$q''_{m,r,i} = U_{isol}(T_{M,r,i} - T_{env}) ; \qquad (22)$$

where q''_m is the heat transferred from the tube wall to the environment, U_{isol} is the global heat transfer coefficient from the tube metal to the environment through the thermal insulation, T_{env} is the environmental temperature. The tube wall temperature, T_M, is calculated by an equation similar to equation (19).

C. Momentum Conservation

For the momentum conservation the difference in the water specific mass through the loop is considered, because in a natural circulation loop the flow is driven by the difference in the fluid density between the ascending and the descending lines. The primary fluid mass flow rate is calculated by the momentum conservation equation, which is written for each pipe segment presented in Fig. 2. For the segment between 4 and 1, corresponding to the ascending line, this equation results in the following:

$$L_{41}\frac{d\dot{m}_p}{dt} = (p_4 - p_1) + \rho_A g(z_4 - z_1) - f_{41}\frac{L_{eq,41}}{D}\rho_A\frac{v_{41}^2}{2} , \qquad (23)$$

where ρ_A is the water specific mass in the ascending line, L_{41} is the pipe length between points 4 and 1, p_4 and p_1 are the pressures in points 4 and 1 respectively, g is the gravity acceleration, z_4 and z_1 are the heights of point 4 and 1 respectively, f_{41} is the friction factor, $L_{eq,41}$ is the equivalent length for the pressure loss, D is the pipe hydraulic diameter (the internal pipe diameter), and v_{41} is the average water velocity between points 4 and 1. Observe that as the overall effect of acceleration along the circuit is canceled, the acceleration terms of the momentum equations were removed.

The momentum equations for the other segments are similar to equation (23). Summing all the momentum equations written for every segment, results in:

$$L\frac{d\dot{m}_p}{dt}=\left(\frac{z_4+z_3}{2}\right)(\rho_A-\rho_D)+\left(\frac{z_1+z_2}{2}\right)(\rho_D-\rho_A)-f\frac{L_{eq}}{D}\rho\frac{v^2}{2}; \quad (24)$$

where L represents the total loop length, ρ_D is the water specific mass in the descending line, and the last term represents the total friction in the loop. The water specific masses in the heat exchanger and in the electric heater are assumed to be an average of the water specific masses in the ascending and in the descending pipes.

D. Cooling Water Control Valve Modeling

The secondary side mass flow rate is modulate by the cooling water control valve. To simulate the cooling water control valve behavior, a generic valve model is considered. This model relates the flow rate to the valve coefficient, C_v. The valve inlet and outlet pressures are considered to be constant, since the flow rate is small and the reservoir water level could be maintained constant. Therefore, the secondary side mass flow rate is given by the following equation:

$$\dot{m}_s=\rho_s A_v \Delta p C_v, \quad (25)$$

where ρ_s is the secondary side water specific mass, A_v is the valve flow area, and Δp is the pressure drop in the valve which is considered constant. The maximum C_v value was experimentally obtained. Its dependence with the valve flow area is modeled by:

$$C_v=(2.7A_v e^{-A_v})C_{v,\max}. \quad (26)$$

E. Numeric Solution, Parameters and NCL Data

The equations that model the thermal and hydraulic processes of NCL are solved with the aid of a computer program. The time derivatives in the dynamic equations are approximated using the Euler Method. Thus, for instance, in the case of the temperatures this approximation yields,

$$T_{r,i}^{t+\Delta t}=T_{r,i}^{t}+\Delta t\frac{\partial T_{r,i}^{t}}{\partial t}; \quad (27)$$

where t is the time and Δt is the integration time step. In the energy equations the space derivatives are approximated by the donor cell method.

The solution of the dynamic processes follows a tandem approach, where the energy equations are solved first (using the previously determined flow rates) followed by the momentum equations. The solution of the energy equations begins at the heat exchanger primary water inlet, in the region numbered R-1. The solution of the energy equations follows the sequence of Fig. 2.

In the momentum equation, the water properties are evaluated at the water mean temperature in each region and not at the conditions in each control volume. As each region is uniformly divided into several control volumes of identical size, the region mean temperature is the arithmetic average of the temperatures of each control volume. The water physical properties are evaluated at these mean temperatures by means of temperature dependent functions.

The friction factor for Reynolds numbers greater than 100 was experimentally obtained, yielding:

$$f=0.7\times\Re e^{-0.25}; \quad (28)$$

for $Re \leq 100$ the friction factor is assumed constant and equal to 0.22.

Fig. 2 shows the NCL primary side divided into eleven (11) regions. Each one of these regions is further divided into the control volumes indicated in the Table 1, inside Fig. 2. This Table also presents the NCL hydraulic data.

As mentioned, the primary and secondary heat transfer coefficients of the heat exchanger and the friction factor correction factor were experimentally obtained. Overall heat transfer coefficients variations within a 15% range were observed in the initial phase of the experiments. This variation is considered small so that constant heat transfer coefficients for both the primary and secondary sides of the heat exchanger are used in the simulations. Table 2 shows the experimental values obtained for these coefficients, note that these values reproduce the experimental global heat transfer coefficient applied to the total heat transfer area (133 W/ °C).

Proceedings of the Eighth International Conference on Nuclear Engineering

ICONE8

"Nuclear Energy in the New Millenium"

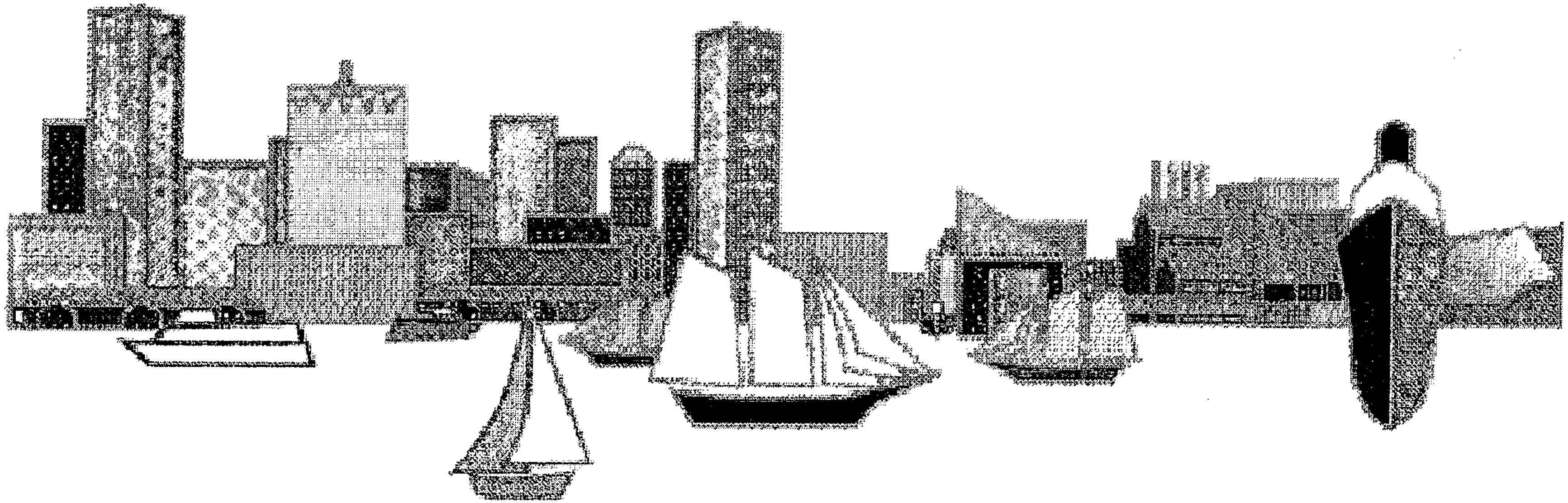

Baltimore, Maryland, USA April 2-6, 2000

Proceed to Table of Contents→